Nonlinear optical properties of ionic magnetic colloids in the femto- and millisecond time scales: change from convergent-to-divergent lens-type behaviors

Diogo Soga and Sarah Alves

Instituto de Física, Universidade de São Paulo, Caixa Postal 66318, 05315-970 São Paulo, São Paulo, Brazil

Alex Campos and Francisco Augusto Tourinho

Instituto de Química, Universidade de Brasília, Caixa Postal 04478, 70919-970 Brasília, Distrito Federal, Brazil

Jerôme Depeyrot

Instituto de Física, Universidade de Brasília, Caixa Postal 04455, 70919-970, Brasília, Distrito Federal, Brazil

Antonio Martins Figueiredo Neto

Instituto de Física, Universidade de São Paulo, Caixa Postal 66318, 05315-970 São Paulo, São Paulo, Brazil

The Z-scan technique is used to measure the nonlinear refractive index n_2 and the nonlinear absorption coefficient β of ionic magnetic colloids as a function of the nanoparticles' diameter (D_{rx}) in the femto- and millisecond time-scale regimes. A change from a convergent-lens type (at a femtosecond time scale) to a divergent-lens type behavior (at a millisecond time scale) is observed. From the values of n_2 and β measured in the femtosecond time-scale regime, the third-order susceptibility $\chi^{(3)}$ is calculated and is shown to depend on D_{rx}: the smaller the D_{rx}, the bigger the $\chi^{(3)}$. A possible origin of the high values of $\chi^{(3)}$ found may be confining effects related to the physical nanoscale of the magnetic particles. © 2006 Optical Society of America

OCIS codes: 160.0160, 190.4400, 190.4720.

1. INTRODUCTION

Different mechanisms can produce nonlinear effects in a material, in particular, changes in its refractive index.[1] Among the mechanisms responsible for these changes, we have the electronic polarization, molecular orientation, electrostriction, saturated and atomic absorption, thermal effects, and photorefractive effects. Each of these mechanisms has a typical time response, ranging from 10^{-15} s (in the case of the electronic polarization) until 10^{-3} s (in the case of thermal effects). These mechanisms can be studied by measuring both the nonlinear refractive index (n_2) and the nonlinear absorption coefficient (β) of the material. In particular, in the case of electronic processes, the third-order nonlinear optical susceptibility ($\chi^{(3)}$) can be calculated from these measured values of n_2 and β.

After the seminal work of Sheik-Bahae *et al.*[2] proposing the Z-scan (ZS) technique, many works were published using it to investigate nonlinear properties of different materials. The ZS technique is used to measure both n_2 and β, and the great advantage of it lies on a very simple setup where a Gaussian profile laser beam is focused by a lens, causing a variation on the beam intensity along the

z direction. The sample, sensitive to the incident laser intensity, is moved through the focused beam path, and the transmitted beam intensity is detected by a photodetector placed behind an aperture. This technique can also be used to probe different nonlinear mechanisms, by adapting the experimental setup to the desired time scale of the phenomenon.

One of the most interesting complex fluids, due to its remarkable physical–chemical properties, is the ferrofluid.[3] This complex fluid is a colloidal suspension of small magnetic particles (typical diameter of ~ 10 nm) dispersed in a liquid carrier (polar or nonpolar, depending on the particular characteristics of the magnetic particles's surface). The fluid is optically isotropic but, in the presence of a small magnetic field (e.g., $\sim 10^2$ G) shows field-induced birefringence and the formation of chains. Moreover, due to its high-magnetic susceptibility, flow properties are strongly dependent on the applied magnetic field. Among the different ferrofluids, the ionics (named here as IF) are particularly interesting[4]: their magnetic particles are electrically charged, to avoid aggregation, and are dispersed in water. Besides their application in the doping of lyotropic liquid crystals,[5] where

their role is to improve the mesophases orientation in small magnetic fields, biocompatible ferrofluids were shown to be a powerful tool in medical therapy.[6]

The nanoscale of the ferrofluid particles, which can be pictured as a dot-type confined system, allows for the interesting study of the nonlinear response of this medium under optical stimuli. The measured third-order nonlinear optical susceptibility of transition metal oxides (α-Fe_2O_3, TiO_2, γ-Fe_2O_3, and Fe_3O_4) in a form of thin films (i.e., a two-dimensional-type confined system) presented values as high as 10^{-12} esu (α-Fe_2O_3) (Ref. 7) to 10^{-10} esu (Fe_3O_4).[8] These values are much bigger than those roughly predicted by using Miller's rule.[9] For example, the predicted value of $\chi^{(3)}$ of Fe_3O_4 is of the order of 3×10^{-13} esu, 3 orders of magnitude smaller than the measured value. ZS experiments in the nanosecond time scale performed with Fe_2O_3-coated nanoparticles dispersed in toluene and hydrosol[10] showed a nonlinear refractive index of the order of -10^{-14} cm^2/W, which gives $|\chi^{(3)}| \sim 10^{-12}$ esu.

In this paper, we used the ZS technique in the femtosecond (fs) and millisecond (ms) time scales to investigate the nonlinear properties of an IF (with uncoated particles), associated to electronic and thermal mechanisms, respectively. The nonlinear refractive indices are measured and the electric susceptibility is evaluated. The third-order nonlinear optical susceptibility of the ferrofluid is compared with those of other confined systems. The paper is organized as follows: in Section 2, both the femtosecond and millisecond formalisms used are presented; in Section 3, the details about the samples and the setups are given, followed by results and discussion in Section 4, and finally the conclusions in Section 5.

2. THEORETICAL BACKGROUND

A. Femtosecond Time-Scale Regime
The induced electric polarization of a medium with inversion symmetry, illuminated by a monochromatic Gaussian laser beam with electric field **E** and frequency w, can be written as: $P^{(3)}(w) = \varepsilon_o X^{(3)}(w;w,-w,w) EE^*E$, where ε_o is the permittivity of free space. The nonlinear refractive index n_2 and the nonlinear absorption coefficient β, in a system whose response is local both in space and time, are defined as: $n(I) = n_o + n_2 I$, and $\alpha(I) = \alpha_o + \beta I$, where $n(I)$ is the refractive index, $\alpha(I)$ is the absorption coefficient, and I is the irradiance (or the intensity), n_o and α_o are the linear index of refraction and absorption, respectively. It is important to notice that, in this time scale (femtoseconds), n_2 has an electronic origin. The real and imaginary parts of the third-order susceptibility are written as

$$\text{Re } \chi^{(3)} = 2n_o^2 \varepsilon_o c n_2 \ [m^2/V^2], \qquad (1)$$

$$\text{Im } \chi^{(3)} = n_o^2 \varepsilon_o c^2 \frac{\beta}{w} \ [m^2/V^2], \qquad (2)$$

where c is the velocity of light in vacuum and w is the frequency of the light. In a ZS experiment, the far-field on-axis irradiance $I(z)$ is measured as a function of sample position (z). For a sample where the nonlinear absorption is small, the on-axis normalized transmittance Γ_N as a function of the sample position z is given approximately by[2,11]

$$\Gamma_N(z) \simeq 1 - \frac{\Delta\Phi_o 4x}{(1+x^2)(9+x^2)} - \frac{\Theta 2(x^2+3)}{(1+x^2)(9+x^2)}, \qquad (3)$$

where $\Delta\Phi_o$ is the on-axis nonlinear phase shift at focus, x is the dimensionless sample position $x = z/z_o$, $\Theta = \beta I_o L_{eff}$, and $z_o = \pi\omega_o^2/\lambda$ is the Rayleigh range of the Gaussian beam with waist ω_o. The nonlinear phase shift $\Delta\Phi_o$ is given by

$$\Delta\Phi_o = -\frac{2\pi n_2 L_{eff} I_o}{\lambda}, \qquad (4)$$

where λ is the wavelength, $L_{eff} = L(1 - e^{-\alpha_o L})/\alpha_o$ is the effective sample thickness, L is the actual sample thickness, and I_o is the on-axis intensity at the focus. The parameter Θ can be measured from the ZS experiments where all the transmitted light (not only the on-axis contribution) is measured by the detector. More details will be given in Section 3. In this case, Eq. (3) is written as

$$\Gamma_N(z) \simeq 1 - \frac{1}{2}\frac{\Theta}{1+x^2}. \qquad (5)$$

B. Millisecond Time-Scale Regime
The nonlinear response of a colloidal medium in the millisecond time-scale regime is studied on the framework of the generalization of the thermal lens model.[12,13] Let us briefly summarize the key points of this analysis. In the time-resolved version of the ZS experiment, a mechanical chopper provides a square-wave light intensity profile, which exhibits a periodical succession of on and off states of equal Δt duration. During an on period, nonlinear effects appear, and temperature T has enough time to reach a steady state in the sample. Conversely, during an off period, no nonlinear effects take place, and the temperature increase has time enough to decay. The sample position z is fixed during a sequence of one on state and one off state. The experiment consists in measuring the sample transmitted intensity [$\Gamma(z,t)$] as a function of time during the on period, at each (fixed) sample position z. The refractive index $n(r,t)$ of the colloidal medium depends on the colloidal particles volume-fraction φ, the temperature T, and the incident light intensity I. All these parameters are functions of the radial distance to the beam axis r and the time t. The variation of the index of refraction $\delta n(r,t)$ can be expressed as the sum of terms arising from the temperature change $\delta T(r,t)$, the particle volume-fraction change $\delta\varphi(r,t)$, and light intensity $I(r,t)$ in the sample, due to the incident beam: $\delta n(r,t) = [\partial n/\partial T]\delta T(r,t) + [\partial n/\partial\varphi]\delta\varphi(r,t) + [\partial n/\partial I]I(r,t)$. Assuming that in this time scale $\delta\varphi \to 0$, i.e., the Soret matter lens has no time to be formed,[13] one has $\delta n(r,t) = [\partial n/\partial T]\delta T(r,t) + n_2^{\dagger}I(r,t)$, where $n_2^{\dagger} = \partial n/\partial I$. It is important to notice that in this time scale (milliseconds), $n_2^{\dagger}$ has a thermal origin. The on-axis optical transmittance $\Gamma(z,t)$ in the far field in a ZS experiment is written as[12]

$$\Gamma(z,t) = \frac{\Gamma'}{1 - 2x\left[\dfrac{C_N}{(1+x^2)^2} + \dfrac{C_T}{1+x^2}\dfrac{t}{t+2t_c}\right] + (1+x^2)\left[\dfrac{C_N}{(1+x^2)^2} + \dfrac{C_T}{1+x^2}\dfrac{t}{t+2t_c}\right]^2},$$ (6)

with $C_N = (8PLz_o n_2^{\dagger})/(\pi\omega_o^4)$ and $C_T = [(\partial n/\partial T)(Lz_o\alpha_o P)]/(\pi\omega_o^2\kappa)$, where Γ' is the sample transmitted intensity when the sample is at $|z|\gg z_o$, at any time $t \leqslant \Delta t$, P and κ are the incident power and the thermal conductivity of the sample, and $t_c = (\omega_o^2[1+x^2])/8D$, with D as the heat diffusivity of the sample. The normalized transmitted intensity $\Gamma_N(z)$ is defined in Eq. (7) and shows a typical peak–valley ZS curve behavior, with a peak-to-valley amplitude defined by Eq. (8):

$$\Gamma_N(z,t \to 0^+) = \frac{\Gamma(z,t \to 0^+)}{\Gamma'} = \Gamma_N(z),$$ (7)

$$\Delta\Gamma_{\mathrm{pv}}^{\mathrm{theo}} = \Gamma_N(z=z_p) - \Gamma_N(z=z_v),$$ (8)

where $t \to 0^+$ is the time corresponding to the first measured transmittance in an on period, z_p and z_v are the peak and valley positions in the ZS curve. This normalization is possible to be done since ferrofluids are strong absorbers, and the nonlinear effects are already present at $t \to 0^+$.[14] In this framework, Eq. (7) may be written as

$$\Gamma_N(z) = \frac{1}{1 - 2x\left[\dfrac{C_N}{(1+x^2)^2}\right] + (1+x^2)\left[\dfrac{C_N}{(1+x^2)^2}\right]}.$$ (9)

3. EXPERIMENTAL

A. Samples
The ferrofluid samples investigated are acid materials (pH=2), with $CoFe_2O_4$ magnetic particles positively charged, dispersed in water. They are labeled IFi ($i=1 \to 4$), as a function of the particles diameter (D_{rx} in nanometers, obtained by x-ray experiments): IF1$\Rightarrow D_{rx}=11.6$; IF2$\Rightarrow D_{rx}=8.8$; IF3$\Rightarrow D_{rx}=7.5$, and IF4$\Rightarrow D_{rx}=4.5$. The ionic water-based ferrofluids elaboration is carried out in three fundamental steps[15]: First, the ferrite nanoparticle synthesis, then the chemical surface treatment, and finally the peptization of the particles in a stable aqueous colloidal dispersion. $CoFe_2O_4$ oxide nanoparticles are prepared using hydrothermal coprecipitating aqueous solutions of a $Co(NO_3)_2$-$FeCl_3$ mixture in an alkaline medium.[16] After the coprecipitation step, the precipitate is washed in order to suppress the high ionic strength of the medium, and the particle surface is cleaned by a $(2 \mathrm{\ mol\ L^{-1}})$ HNO_3 solution. Moreover, to obtain the thermodynamical stability of the particles, an empirical process is used: the precipitates are boiled with a 0.5 mol L^{-1} $Fe(NO_3)_3$ solution. Then, the particles are conveniently peptized in an acidic medium by adjustment of the ionic strength, resulting in a stable sol of high quality. The crystalline structure and the mean size of our magnetic nanoparticles were carried out from x-ray diffraction measurements performed on powder samples, at 25 °C,

obtained after evaporation of the liquid carrier. The chemical composition of the synthesized nanoparticles was checked: the concentrations of Fe and Co ions were determined by inductively coupled plasma atomic emission spectroscopy (ICP-AES). Then, the volume fractions of the magnetic material φ of all precursor samples were deduced. In the following experiments, the precursor dispersions were diluted in order to obtain samples whose volume fractions are sufficiently low ($\varphi \sim 1\%$) to neglect the magnetic dipolar interaction between particles. In the ZS experiments, all the samples are encapsulated between optical glass plates with dimensions (20 mm $\times$ 10 mm $\times$ 1 mm), with a Teflon spacer $L=24\ \mu$m thick. The values of φ are chosen by analyzing the transmittances and the sample response to the incident laser beam. $\varphi_{\min}$ is the minimum volume fraction of the magnetic material, that gives a good signal-to-noise ratio in the ZS experiment, with the maximum available beam power. $\varphi_{\max}$ is the maximum volume fraction of magnetic material that does not show thermal-induced hydrodynamic instabilities in the sample due to the laser heating, at the lowest value of the beam power. So, we chose $\varphi_{\min} < \varphi < \varphi_{\max}$. All the measurements were performed at $T = 20$ °C.

B. Linear Optical Absorption and Linear Refractive Index
The linear optical absorption (α_o) of the samples is measured with a UV-2800 single beam scanning UV–Visible spectrophotometer (at $\lambda_s=532$ nm). The linear refractive index (n_o) of the different samples (at $\lambda_r=589$ nm) is measured using an Abbe refractometer (Carl Zeiss) with a temperature controlled device (thermal bath Brookfield TC 500 with 0.01 °C accuracy).

C. Z-Scan Apparatus and Technique
1. Femtosecond Time-Scale Setup
A mode-locked Ti:sapphire laser ($\lambda=790$ nm), pumped by a 5 W cw doubled frequency Nd:YVO$_4$ ($\lambda_p=532$ nm) laser, is used in these ZS experiments. The pulse width is of 508.5 fs, and the irradiance on the sample ranges from 0.16 to 0.22 GW/cm^2. By using a pulse selector, the femtosecond pulses are separated (peak-to-peak) in time by 240 ns (originally, without the pulse selector, the Ti:sapphire pulse frequency is 82 MHz). A lens of focal distance $f=88.3$ mm, which provides a minimum waist of $\omega_o = 27.3\ \mu$m, with a Rayleigh length $z_o=2.97$ mm, is placed before the sample. The sample is put in the beam path and is moved around $z=0$, before and after the focal point, along the z axis. The transmitted beam goes to the detector and is recorded by an oscilloscope. The beam intensity I at a point z changes due to a change of the beam waist $[\omega(z)]$. This intensity I reaches the maximum value at the focal point, then it decreases for far points. The optical

nonlinear characteristics of the sample arise mainly near $z = 0$ due to high intensity I, and at far points, it is not noticeable. For the measurement of the nonlinear refractive index only the on-axis transmittance is measured. On the other hand, to measure the nonlinear absorption, a converging lens is placed after the sample to collect all the transmitted beam at the detector. The incident (peak) laser power used in each experiment is $I_o \sim 10^{12}$ W/m^2.

2. Millisecond Time-Scale Setup
In the time-resolved version of the ZS experiment, a mechanical chopper modulates the laser beam (Gaussian profile) providing a square-wave pulse, which exhibits a periodical succession of on and off states of equal Δt duration. The sample position z is fixed during a sequence of one on state and one off state. The experiment consists of measuring the sample transmitted intensity ($\Gamma(z,t)$) as a function of time during the on period at each (fixed) sample position z. A cw doubled frequency Nd:YVO$_4$ (λ = 532 nm) laser is used in the ZS measurements. The laser beam is chopped (at 18 Hz) or controlled by a shutter for larger time intervals Δt and focused by a lens (focal distance $f = 100$ mm), which provides a minimum waist of $\omega_o = 20.3$ μm, with a Rayleigh length $z_o = 2.43$ mm. The time resolution in the experiment is ~ 100 μs, and the ZS step used is $\Delta z = 0.5$ mm. For each ZS measurement, the sample is placed in a chariot, which moves it along the z axis of the laboratory frame, with its largest surface perpendicular to the laser beam. Depending on the magnetic particle concentration, different incident beam powers are used in the experiments. A sketch of the experimental setup can be found in Ref. 12.

4. RESULTS AND DISCUSSION

A. Femtosecond Time-Scale Processes
Figure 1 shows typical on-axis [Fig. 1(a)] and total [Fig. 1(b)] ZS transmittances as a function of z of the ionic IF2 magnetic colloid. Each point represents the average of five independent measurements. The solid curves represent the best fits of Eqs. (3) and (5), respectively, to the experimental data. From these fittings, the parameters n_2 and β can be obtained. Their values for the set of samples investigated are given in Table 1. The order of magnitude of n_2 obtained in our experiment (10^{-11} cm^2/W) clearly indicates that the mechanism responsible for this response is not thermal.[1] This order of magnitude is ten times smaller than that found in chitosan/CdSe-ZnS quantum dot (QD) core-shell multilayer films (at the same wavelength), where the typical diameters of the CdS and ZnS QDs were ~ 4 nm, and the film thickness per bilayer ~ 8 nm.[17]

With our measured values of n_2 and n_o ($= 1.328 \pm 0.002$), it is possible to calculate the real part of the third-order nonlinear electric susceptibility of the samples using Eq. (1). These values are presented in Table 1. To check if we are really probing Re $\chi^{(3)}$ and not high-order susceptibilities, we performed the ZS experiment with three different incident (peak) laser powers: $I_o = 3.87$, 4.04, and 4.71 ($\times 10^{11}$ W/m^2). The variation in the values of n_2 obtained was smaller than 3% indicating that our ZS experiment measures Re $\chi^{(3)}$ and not high-
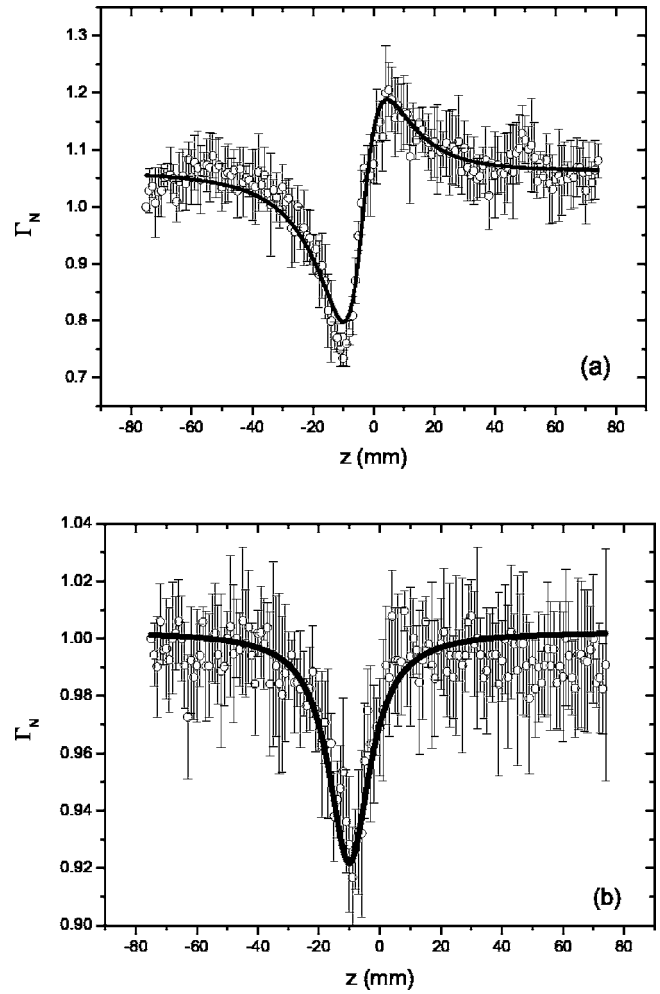

Fig. 1. Typical ZS curves of the normalized transmittances in the femtosecond experiment, as a function of z. Water-based ionic sample IF2: (a) on-axis transmittance. The solid curve represents the best fit of Eq. (3) to the experimental data (b) Total transmittance. The solid curve represents the best fit of Eq. (5) to the experimental data.

Table 1. Femtosecond ZS Experiment Results[a]

Label	n_2 (10^{-11} cm^2/W)	β (10^3 cm/GW)	Re $\chi^{(3)}$ (10^{-17} m^2/V^2)	Im $\chi^{(3)}$ (10^{-18} m^2/V^2)
IF1	2.1 ± 0.2	2.7 ± 0.1	2.0 ± 0.2	1.6 ± 0.4
IF2	2.4 ± 0.1	3.22 ± 0.06	2.2 ± 0.1	1.9 ± 0.5
IF3	2.7 ± 0.2	5.3 ± 0.6	2.6 ± 0.2	3.1 ± 0.9
IF4	3.5 ± 0.3	9.0 ± 0.5	3.2 ± 0.3	5 ± 1

[a]Label of the investigated magnetic colloidal samples, nonlinear index of refraction (n_2), nonlinear optical absorption (β), and real and imaginary parts of $\chi^{(3)}$.

order susceptibilities. The sign of n_2 is positive, indicating a convergent-lens-type behavior at this time-scale regime.

The order of magnitude of β found in our experiments is $\sim 10^3$ cm/GW. This order of magnitude is also the same found in chitosan/CdSe-ZnS core-shell QD multilayer films. The value of β for this multilayer film is much larger than that in the bulk CdSe (~ 6.4 cm/GW). As likely as in the case of the multilayer QDs, confining effects in our nanoparticles seem to be responsible for this order of magnitude of β found in our samples. We will

come back to this point in the following sentences. Different from the case of n_2, the same experiment performed at different values of I_o shows a variation of about 30% in the value of β, in the range of intensities investigated (Fig. 2). This fact indicates that, besides $\chi^{(3)}$, high-order susceptibilities have been probed in our ZS experiment to determine β. However, we can evaluate the order of magnitude of the imaginary part of $\chi^{(3)}$ using Eq. (2) and $w = 2.386 \times 10^{15}$ Hz, being Im $\chi^{(3)} \sim 10^{-18}$ m^2/V^2. This problem, in the determination of the Im $\chi^{(3)}$ by using the ZS technique and the procedure described here, is expected because when the total transmitted intensity is collected by the lens and measured by the detector, not only may we collect the contribution from the third-order susceptibility, but also we may collect the high-order contributions (if present). This fact limits the application of the ZS technique for this particular measurement.[18]

The modulus of $\chi^{(3)}$, evaluated from our data, is shown in Fig. 3, being of the order of 10^{-17} m^2/V^2 (or, 10^{-9} esu): the smaller the magnetic particle diameter, the bigger the modulus of $\chi^{(3)}$. It is interesting to compare these values with those of other confined systems. In the case of the sol–gel derived α-Fe$_2$O$_3$, γ-Fe$_2$O$_3$, and Fe$_3$O$_4$ thin films (a two-dimensional-type confined system), $\chi^{(3)}$ are 5.8 $\times 10^{-11}$ esu, 2.1×10^{-11} esu, and 4×10^{-10} esu, respectively.[8] These are the highest values among inorganic oxides. In the case of the α-Fe$_2$O$_3$ and γ-Fe$_2$O$_3$, these high values were attributed to the pair excitation process while, in the case of the Fe$_3$O$_4$, it was attributed to both one-photon and three-photon resonances. Fe$_2$O$_3$-coated nanoparticles dispersed in toluene and hydrosol[10] presented $|\chi^{(3)}| \sim 10^{-12}$ esu. In our IF colloidal system, the magnitude of $\chi^{(3)}$ is 2 orders of magnitude bigger than that of the α-Fe$_2$O$_3$ and γ-Fe$_2$O$_3$ and, in the case of the Fe$_3$O$_4$, 1 order of magnitude bigger. A possible origin of the high values of $\chi^{(3)}$ found in IF may be confining effects related to the physical nanoscale of the magnetic particles. This hypothesis is reinforced by the dependence of $\chi^{(3)}$ with the particle's diameter (Fig. 3). The IF shows the highest $|\chi^{(3)}|$ among other two-dimensional (thin films) and dot-type (coated nanoparticles) confined sys-
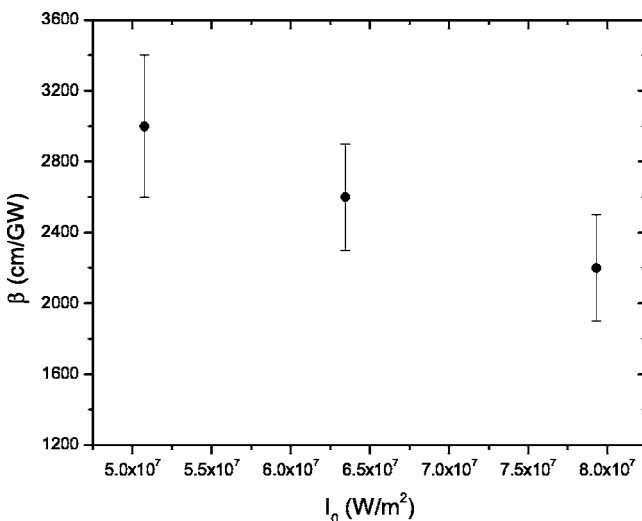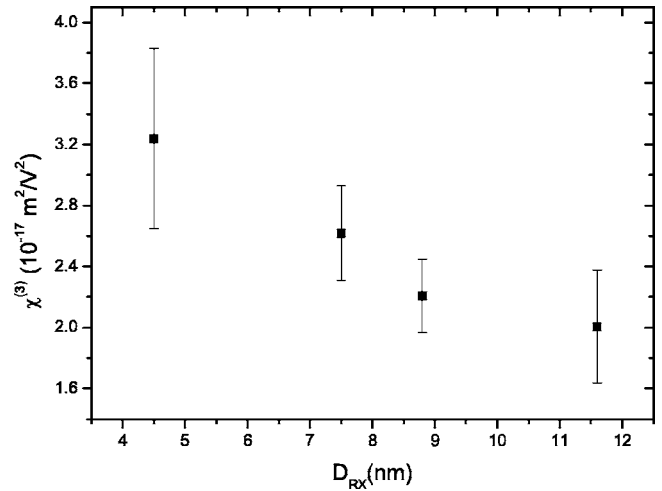

Fig. 3. Modulus of $\chi^{(3)}$ as a function of the magnetic particle's diameter. Water-based ionic sample IF2.

Table 2. Millisecond ZS Experiment Results^a

Label	$-n_2^{\dagger}$ (10^{-7} cm^2/W)	α_o (cm^{-1})
IF1	2.76 ± 0.14	205.75 ± 0.32
IF2	2.30 ± 0.11	201.01 ± 0.45
IF3	1.80 ± 0.09	196.07 ± 0.51
IF4	1.46 ± 0.07	98.15 ± 0.11

^{a}Label of the investigated magnetic colloidal samples, nonlinear index of refraction ($n_2^{\dagger}$), and linear light absorption coefficient at 532 nm (α_o).

tems. Different from the case of the Fe$_2$O$_3$-coated nanoparticles, our particles are uncoated but are electrically charged.

B. Millisecond Time-Scale Processes
As pointed out at the end of Section 2, the data treatment proposed at this time scale is adequate to strong absorbers. To check the hypothesis that ferrofluids fulfill this condition, the linear light absorption coefficient (α_o) of the different samples is measured, and the values are given in Table 2. These values (of the order of 10^2 cm^{-1}) support the theoretical framework used to analyze the ZS curves following the normalization procedure present in Eq. (7).

Figure 4 shows typical on-axis ZS transmittance as a function of z of the ionic IF2 magnetic colloid. Each point represents the average of five independent measurements. The data treatment to obtain the values of $n_2^{\dagger}$ from the ZS curves is described in detail in Refs. 13 and 14. The dimensionless parameter C_N is obtained by means of a master curve, and knowing P, L, z_o, and ω_o, we can calculate $n_2^{\dagger}$. Within our accuracy, any nonlinear absorption is found in all the IF samples investigated (data not shown), in this time-scale regime.

Different, from the femtosecond time-scale regime, $n_2^{\dagger} < 0$, its order of magnitude is 10^{-7} cm^2/W, which is characteristic of a thermal mechanism. $n_2^{\dagger}$ depends on the magnetic particle's diameter: the smaller the D_{rx}, the smaller the absolute value of $n_2^{\dagger}$ (Fig. 5). The sign of $n_2^{\dagger}$ is negative, indicating a divergent-lens-type behavior at this time-scale regime. Since the magnetic particles are strong absorbers at this wavelength, it is expected that they in-

Fig. 2. Nonlinear optical absorption β as a function of the incident (peak) laser power I_o. Water-based ionic sample IF2.

crease their temperature due to the laser-light absorption and transfer this heat to the fluid carrier, in this case, the water. This mechanism increases locally the sample temperature imposing a modification of its local density, originating the divergent-lens-type effect. In this sense, the larger surface area of the larger particles favors the heat conduction from them to the carrier fluid (i.e., the water), which is responsible for the local density modifications of the sample under the laser illumination.

5. CONCLUSIONS

The Z-scan technique is used to measure the nonlinear refractive index and the nonlinear absorption coefficient of ionic magnetic colloids as a function of the nanoparticles' diameter in the femto- and millisecond time-scale regimes. In the femtosecond regime, the magnetic colloids show a convergent-lens-type behavior, and, at this time scale, the processes responsible for the systems' optical response are expected to be from electronic origin. Both n_2 and β were shown to depend on the particles' diameter: the smaller the particle's diameter, the bigger n_2 and β.
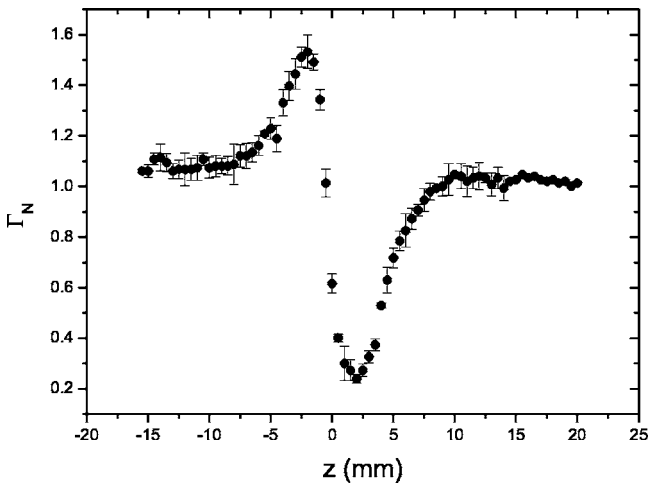

Fig. 4. Typical ZS curve of the normalized transmittances in the millisecond experiment, as a function of z. Water-based ionic sample IF2.
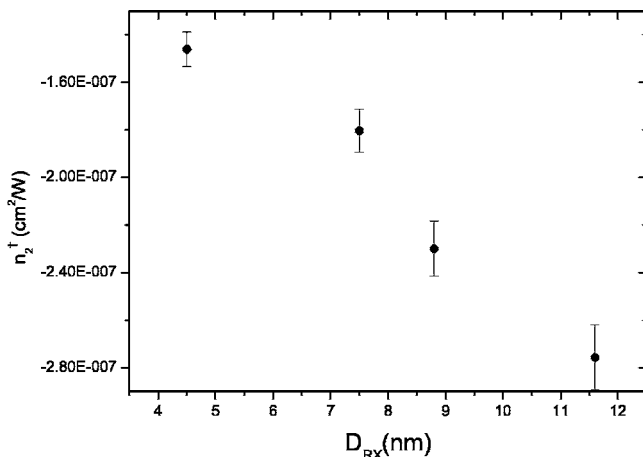

Fig. 5. Nonlinear refraction index $n_2^\dagger$ as a function of the magnetic particle's diameter D_{rx}.

From these values, the third-order susceptibility $\chi^{(3)}$ could be calculated and showed the same type of behavior with respect to the magnetic nanoparticles' diameter. A possible origin of the high values of $\chi^{(3)}$ found in ionic ferrofluids may be confining effects related to the physical nanoscale of the magnetic particles. The ionic ferrofluid shows the highest $|\chi^{(3)}|$ among other two-dimensional (thin films) and dot-type (coated nanoparticles) confined systems. When the systems are investigated in the millisecond time-scale regime, the magnetic colloids show a divergent-lens-type behavior, and $|n_2^\dagger|$ is smaller for systems with the smallest nanoparticle diameter. At this time scale, the processes responsible for the systems' responses are from thermal origin.

REFERENCES

1. R. W. Boyd, *Nonlinear Optics* (Academic, 1992).
2. M. Sheik-Bahae, A. A. Said, and E. W. Van Stryland, "High sensitivity single-beam n_2 measurements," Opt. Lett. **14**, 955–957 (1989).
3. R. E. Rosensweig, *Ferrohydrodynamics* (Cambridge U. Press, 1985).
4. R. Massart, "Preparation of aqueous magnetic liquids in alkaline and acid media," IEEE Trans. Magn. **17**, 1247–1248 (1981).
5. A. M. Figueiredo Neto and S. R. A. Salinas, *The Physics of Lyotropic Liquid Crystals: Phase Transitions and Structural Properties* (Oxford U. Press, 2005).
6. J. W. M. Bulte, "Magnetic nanoparticles as markers for cellular MR imaging," J. Magn. Magn. Mater. **289**, 423–427 (2005).
7. T. Hashimoto, T. Yoko, and S. Sakka, "Third-order nonlinear optical susceptibility of α-iron (III) oxide thin film prepared by the sol–gel method," J. Ceram. Soc. Jpn. **101**, 64–68 (1993).
8. T. Hashimoto, T. Yamada, and T. Yoko, "Third-order nonlinear optical properties of sol–gel derived α-Fe$_2$O$_3$, γ-Fe$_2$O$_3$, and Fe$_3$O$_4$ thin films," J. Appl. Phys. **80**, 3184–3190 (1996).
9. C. C. Wang, "Empirical relation between the linear and the third-order nonlinear optical susceptibility," Phys. Rev. B **2**, 2045–2048 (1970).
10. B. Yu, C. Zhu, F. Gan, X. Wu, G. Zhang, G. Tang, and W. Chen, "Optical nonlinearities of Fe$_2$O$_3$ nanoparticles investigated by Z-scan technique," Opt. Mater. **8**, 249–254 (1997).
11. H. J. Yuan, L. Li, and P. Palffy-Muhoray, "Nonlinear birefringence of nematic liquid crystals," Proc. SPIE **1307**, 363–373 (1990).
12. S. Alves, A. Bourdon, and A. M. Figueiredo Neto, "Generalization of the thermal lens model formalism to account for thermodiffusion in a single-beam Z-scan

experiment: determination of the Soret coefficient," J. Opt. Soc. Am. B **20**, 713–718 (2003).

13. S. Alves, F. L. S. Cuppo, and A. M. Figueiredo Neto, "Determination of the nonlinear refractive index of lyotropic mixtures with and without the ferrofluid doping: a time-resolved Z-scan experiment in millisecond time scales," J. Opt. Soc. Am. B **23**, 67–74 (2006).

14. S. Alves, A. Bourdon, and A. M. Figueiredo Neto, "Investigation of the Soret coefficient in magnetic fluids using the Z-scan technique," J. Magn. Magn. Mater. **289**, 285–288 (2005).

15. M. H. Sousa, J. Depeyrot, G. J. da Silva, M. C. F. L. Lara, and F. A. Tourinho, "New electric double-layered magnetic

fluids based on copper, nickel, and zinc ferrite nanostructures," J. Phys. Chem. B **105**, 1168–1175 (2001).

16. F. A. Tourinho, R. Franck, and R. Massart, "Aqueous ferrofluids based on manganese and cobalt ferrites," J. Mater. Sci. **25**, 3249–3254 (1990).

17. X. Wang, Y. Du, S. Ding, Q. Wang, G. Xiong, M. Xie, X. Shen, and D. Pang, "Preparation of third-order optical nonlinearities of self-assembled chitosan/CdSe-ZnS core-shell quantum dots multilayer films," J. Phys. Chem. B **110**, 1566–1570 (2006).

18. F. Yoshino, S. Polyakov, M. Liu, and G. Stegeman, "Observation of three-photon enhanced four-photon absorption," Phys. Rev. Lett. **91**, 0639021 (2003).